New Analytical Model for Load distribution and Pitting Stress analysis of a Spur Gear on Lathe Machine

Khin Khin Thant
Department of Mechanical Engineering
Yangon Technological University (YTU)
Yangon, Myanmar
Kkhinthant35@gmail.com

Than Than Htike
Department of Mechanical Engineering
Yangon Technological University (YTU)
Yangon, Myanmar
drthanthan.mech@gmail.com

Abstract

Gears are an important part of mechanical power transmission. There are two main types of spur gear stresses. They are pitting stress (contact stress) and bending stress. If both teeth are in contact and rotate, the gear will fail due to this pitting stress. To reduce this stress, a model is presented to calculate the strength of a gear pair. The load distribution ratio between the pairs of teeth in contact is determined by the contact ratio and the position of the contact point. The magnitude of the stress along the contact line is calculated using Hertz contact equation AGMA contact equation, and the load distribution along the contact line is determined by the criterion of the minimum elastic potential. Finally, the results of the spur gear stresses were obtained from four different parameters with MATLAB and compared with the allowable contact stresses.

Keywords: Contact stress, Different parameters, Load distribution, MATLAB software, Spur gear

1. Introduction

Gears are the most common means of transmitting power in the modern mechanical engineering world. They vary from a tiny size used in watches to the large gears used in lifting mechanisms and speed reducers. They form vital elements of main and many machines such as automobiles, tractors, milling machines etc. Toothed gears are used to change the speed and power ratio as well as the direction between input and output. Gears are the most common way of transmitting energy in the world of modern mechanical engineering. It ranges from the small size used in clocks to the large gears used in hoists and speed reducers. It is an essential element in basic machines and many of them, such as cars, tractors, lathe machines and others. The gears are used to change the ratio of speed and power, as well as the direction between the input and the output.

Load distribution models for external gears, based on the minimum elastic potential energy criterion, were developed by the authors in previous works [1]. Wang and Zhang [2] calculated the stiffness of dental tissue based on the Hertz model of a linear relationship between cylinders. In all cases, the results are satisfactory, so it can be concluded that the Hertz equation for the contact between two cylinders accurately describes the contact between the tooth surfaces, which are calculated by integrating the theoretical elasticity equation as a function of the normal load. The potential elastic energy of a pair of teeth at any contact position on the contact path is calculated by integrating the theoretical elasticity equation as a function of normal load. This formula allows to express the shared load ratio using simple analytical equations that facilitate the study of maximum stress and load capacity. Contact stiffness is not difficult to account for, assuming that the Hertzian contact pattern between the two cylinders is accurate enough to describe the contact between the involute teeth. In fact, the deviation of stiffness in Hertz between the two cylinders is proportional to the total transmitted load, which means load independent stiffness. The contact between the surfaces of the spur gear is in a straight line parallel to the axis of rotation of the gear, and all the points of contact on each

surface have the same radius of curvature. Since this contact state is very similar to contact between two cylinders, the Hertz model must be accurate.

A load distribution model for external gears was developed on minimum elastic potential energy criteria of four different parameters (i.e., change the normal modules, change the addendum factors, change the fillet radii, change the normal pressure angles). This job was to establish an empirical pinion relationship to reduce the pitting stress induced in the pinion geometry at the point of contact. Loads are applied along the contact position and the highest single tooth contact point (HPSTC).

The main objective of this work was to establish an empirical relationship to predict the percentage reduction of pitting stress in cylindrical gears by using four different methods. Develop efficient and reliable programs in MATLAB. The data obtained from this analysis was used in lathe machine to compare with the allowable contact stresses. The presents a spur gear model with load distribution at the contact point. Equations fitted for inverse units for unit face width are also presented. This equation is simple, accurate, and depends on the contact ratio relationship. Using this equation, the load distribution coefficient and, consequently, the load at any point in the contact path was determined, for both standard and various parameters of a spur gear transmission. The calculated of the critical contact stress, load distribution conditions and reduces the fracture site using four different spur gear parameters.

2. Classification of gear

Generally, gears are categorized into three distinct types based on relative positions of axes of shafts: (i) The transmission of power and motion between the parallel shafts [3]. For example: Spur and Helical gears. (ii) The transmission of power and motion between those shafts whose axes are intersecting and angle between them is 90°. For example: Bevel and Spiral bevel gears (iii) The transmission of power and motion between those shafts which neither parallel nor intersecting the angle between axes is 90° but they are in different planes. For example: Worm and Worm wheel, Crossed helical gears, Hypoid gears [4].

3. Contact ratio

The contact ratio is obtained as the ratio between the working length and the reference pitch shown in fig.1. Gears typically have a contact ratio of 1.4 to 1.8. The contact coefficient is 1.6, which means that in 40 percent of cases one pair of teeth will be in contact and in 60 percent of cases there will be two pairs of teeth in contact [5].

The contact ratio can be calculated as follow:

$$\text{contact ratio}, \varepsilon_\alpha = \frac{\text{Length of action}, L_{ab}}{\text{base pitch}, P_b}$$

$$\varepsilon_\alpha = \frac{\sqrt{r_{a1}^2 - r_{b1}^2}}{\pi m \cos\alpha} + \frac{\sqrt{r_{a2}^2 - r_{b2}^2}}{\pi m \cos\alpha} - \frac{(r_1 + r_2)\sin\alpha}{\pi m \cos\alpha} \quad (1)$$

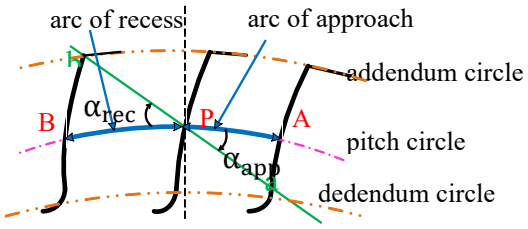

Figure.1 Contact ratio

The existing data and material properties of spur gears used in lathe machine are shown in Table 1 and Table 2.

Table 1. Existing data for spur gears

No	Input Parameter	Pinion	Gear
1	Number of teeth	40	127
2	Face width	15mm	15mm
3	Module	1.25	1.25
4	Maximum Torque	30 Nm	-
5	Rotational speed	440 rpm	-
6	Pressure angle	20 deg full depth	
7	Profile	involute	Involute

Table 2. Material properties of spur gears

No	Name	Symbol	Value
1	Material	AISI-4140	-
2	Ultimate strength	σ_u=1075	MPa
3	Yield Strength	σ_y=986	MPa
4	Modulus of Elasticity	E=190	GPa
5	Poisson's ratio	μ=0.29	-
6	Brinell hardness of material	H_B=311	-

4. Load distribution model

The load distribution model is used to determine minimum elastic capacity. The elastic potential energy u is calculated from the theoretical equations of elasticity and tooth geometry. For calculations, spur gears with specific loads and face width are taken into account. Its elastic potential u is called the unit potential, and its inverse unity potential $v = u^{-1}$ depends on the contact point, which is described by the contact point parameter ξ in the gear profile:

$$\xi_c = \frac{z}{2\pi}\sqrt{\frac{r_c^2}{r_b^2} - 1} \tag{2}$$

where z is the number of teeth, r_c the radius of the contact point, r_b the base radius and subscript 1 denotes the pinion (subscript 2 will denote the wheel) as shown in fig.2. [6]. Note that the difference of ξ parameters corresponding to contact at the outer point of contact and at the inner point of contact is equal to the transverse contact ratio ε_α. Similarly, the difference in the parameters ξ corresponding to two teeth connected in simultaneous contact is 1. For cylindrical gears, the elastic potential energy is calculated taking into account all pairs of teeth in simultaneous contact.

$$\xi_w - \xi = \lambda = \frac{z_2 - z_1}{2\pi}\tan\alpha \tag{3}$$

Where, α is the operating pressure angle,

λ is the distance between both tangency points divided by the pinion base radius and the pinion angular pitch.

The load distribution ratio of a spur gear should be the same as that of an uncut gear, except for the inner contact point and the outer contact point of the pair of teeth, which are offset to the right by an equal. With a linear variation in the ratio of the load distribution over the contact interval of two pairs of teeth, the ratio of the load distribution can be expressed as:

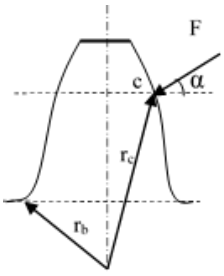

Fig.2 Geometry of involute external teeth.

$$R(\xi)=0.35+0.3\frac{\xi-\xi_{inn}}{\varepsilon_\alpha-1} \quad \text{for } \xi_{inn}\le\xi\le\xi_{inn}+\varepsilon_\alpha-1$$
$$R(\xi)=1 \quad \text{for } \xi_{inn}+\varepsilon_\alpha-1\le\xi\le\xi_{inn}+1 \tag{4}$$
$$R(\xi)=0.65-0.3\frac{\xi-\xi_{inn}}{\varepsilon_\alpha-1} \quad \text{for } \xi_{inn}+1\le\xi\le\xi_{inn}+\varepsilon_\alpha$$

These equations are very simple and accurate enough to calculate resistance and easily determine critical stresses and loading conditions. Although the expected discrepancies with the results published in [7] are small, the analysis can be carried out without difficulties.

However, Figure 2 offers to find an approximate equation for similar ξ using the equation. (2). To validate Equations. (2) and (3) and the load distribution obtained from the combination of these equations with Eq. (4) have been carried out for standard contact ratio spur gears, and various contact ratio spur gears using different parameter.

To prove for small discrepancies between models, load sharing ratios were examined on a standard single point gear ratio (inner and outer of contact points, as well as points inner and outer of contact range single tooth) of focus. The following geometry values, but ignore the case of undercut gear profiles:

Case.1 Module, m: 1.25, 1.375,1.5.

Case.2 Addendum factor, a:1m,1.05m,1.1m,

Case.3 Pressure angle, α: 19°, 20°, 21°.

Case.4 Fillet radius, r_f: 0.3m, 0.4m, 0.5m.

4.1. Case.1 change the module

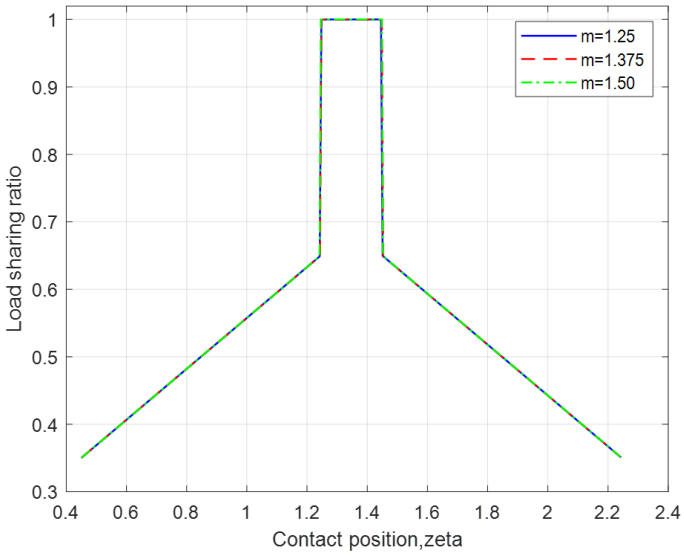

Fig. 3 Load distribution for increased the module

4.2. Case.2 change the addendum factor

The results obtained from the analytical method are described above. For the modules of 1.25, 1.375 and 1.5, the distributions of load sharing ratio along the contact position are shown in Figure 3. The load sharing ratio are constant until the module changes. The load sharing ratios are symmetric.

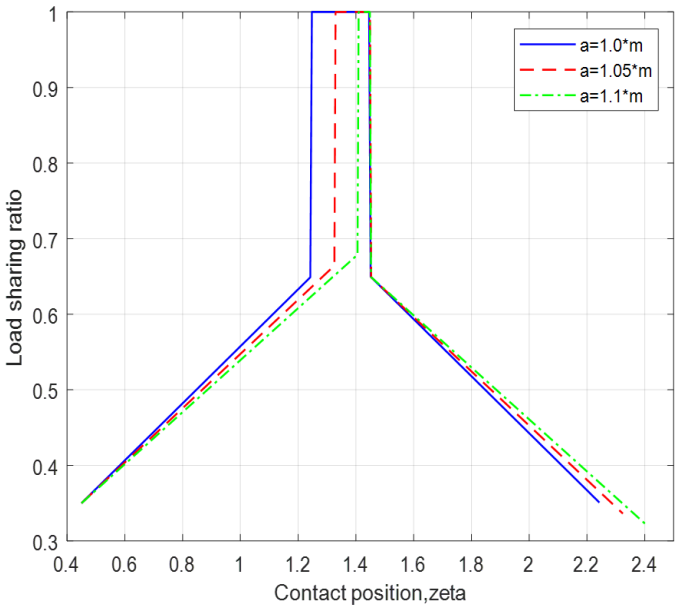

Fig.4 Load distribution for increased the addendum factor

4.3. Case.1 change the fillet radius

The results obtained from the analytical method are described above. The distribution of load sharing ratio along the contact position for the addendum factor of 1.0*m,1.05*m and 1.1*m are shown in Figure 4. The maximum load sharing ratio position is reduced due to increasing the addendum factor. The load sharing ratio are unsymmetrical.

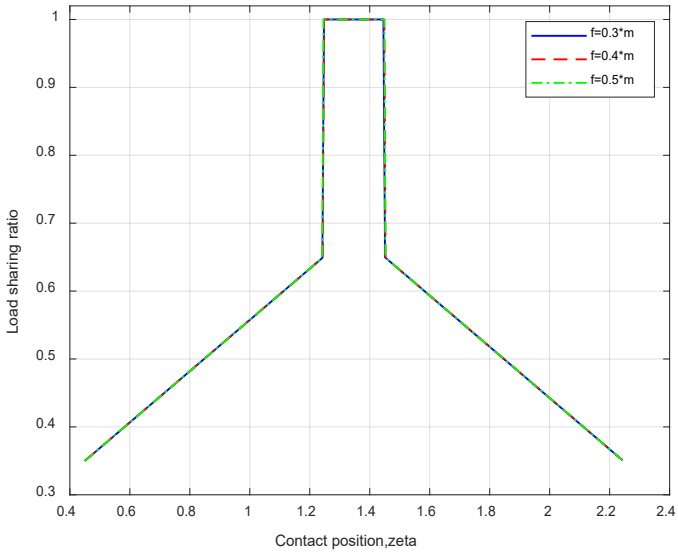

Fig. 5 Load distribution for increased the fillet radius

The results obtained from the analytical method are described above. The distributions of load sharing ratio along the contact position for the fillet radius of r_f=0.3*m, r_f=0.4*m, and r_f=0.5*m are shown in the Figure 5. The load sharing ratios are constant until the fillet radius changes. The load sharing ratios are symmetric.

4.4. Case.1 change the pressure angle

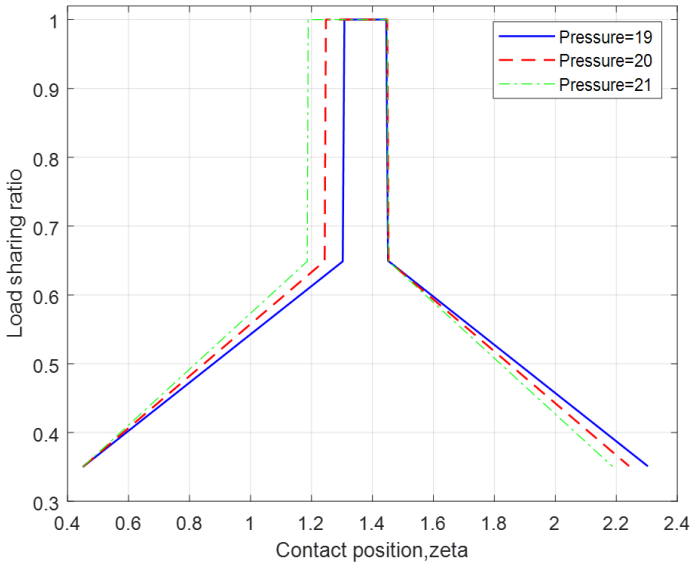

Fig.6 Load distribution for changed the pressure angle

The results obtained from the analytical method are described above. The distributions of load sharing ratio along the contact position for the pressure angles of 19°.20°, and 21° are shown in the Figure 6. The maximum load sharing ratio position is reduced due to reducing the pressure angle. The load sharing ratio are symmetric.

5. Contact stress (Pitting stress)

To compute the pitting load capacity of spur gears, all the gear rating standards [8] can be evaluated using contact stress with the Hertz equation. It can be written as:

$$\sigma_H = Z_E \sqrt{\frac{F}{b} R(\xi) \frac{1}{\rho(\xi)}} \tag{5}$$

Where, Z_E is the elasticity factor (according to ISO 6336–2 [9]) and

$\rho(\xi)$ is the relative curvature radius of the involute profiles of the pinion and wheel

ξ. is the contact point position

Obviously, the pitting load capacity will be determined by the maximum value of the contact stress along the path of contact, which should be calculated. Z_E depends on the modulus of elasticity E and the Poisson's ratio υ of the material of each gear, and is given by

$$Z_E = \left[\pi \left(\frac{1-\upsilon_1^2}{E_1} + \frac{1-\upsilon_1^2}{E_1} \right) \right]^{-\frac{1}{2}} \tag{6}$$

The relative curvature radius can be derived from:

$$\rho(\xi) = \pi m \cos\alpha \frac{\xi(\lambda+\xi)}{\lambda} \tag{7}$$

Where, m is the normal module. The load per unit of length can be expressed as:

$$f(\xi) = \frac{F}{b} R(\xi) \tag{8}$$

5.1.Case.1 Hertz's contact stress changes the modules

The results showed that the stress distribution along the contact position was found in three different modules. The distribution of pitting stress is slowly decreased at the base of gear tooth; the maximum pitting stress occurs at the middle portion of the gear tooth, and the pitting stress is reduced at the tip of the gear tooth is shown in Figure 7. The gear failure occurs at the middle portion of the gear tooth because the maximum pitting stress appears in this position. If the module is increased, the pitting stress along the pinion tooth is reduced but it can be increased the weight of gear.

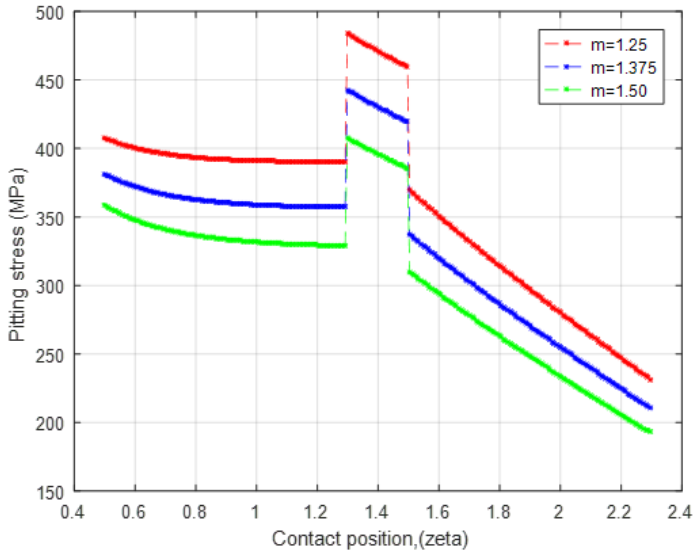

Fig. 7 Pitting stress along the pinion tooth

5.2. Case.2 Hertz's contact stress changes the addendum factors

The results showed that the stress distribution along the contact position was found in three different addendum factors. The distribution of pitting stress is slowly decreased at the base of gear tooth; the maximum pitting stress occurs at the middle portion of the gear tooth, and the pitting stress is reduced at the tip of gear tooth is shown in Figure 8. The gear failure is occurred at the middle portion of gear tooth because the maximum pitting stress is appeared in this position. If the addendum factor is increased, the pitting stress along the pinion tooth is reduced as the maximum contact position is reduced.

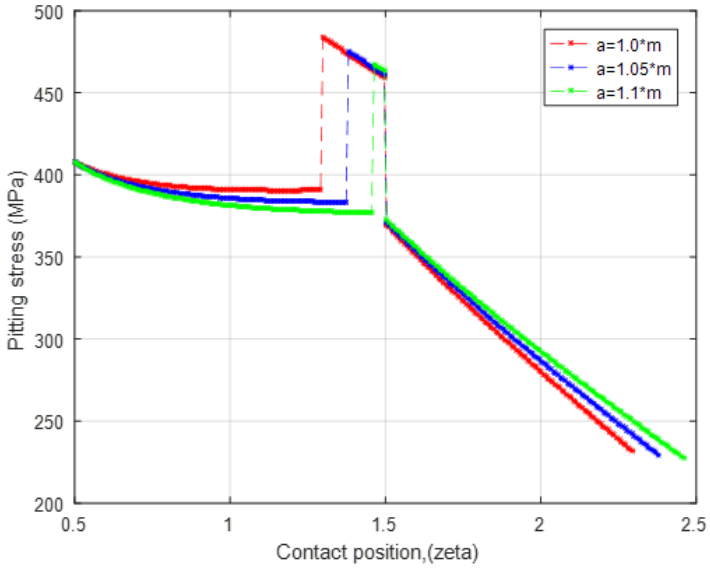

Fig. 8 Pitting stress along the pinion tooth

5.3. Case.3 Hertz's contact stress changes the fillet radius

The results showed that the stress distribution along the contact position was found in three different fillet radii. The distribution of pitting stress is slowly decreased at the base of the gear tooth, the maximum pitting stress occurs at the middle portion of the gear tooth, and the pitting stress is reduced at the tip of the gear tooth is shown in Figure 9. Although the fillet radius increase, the pitting stress along the pinion tooth is constant.

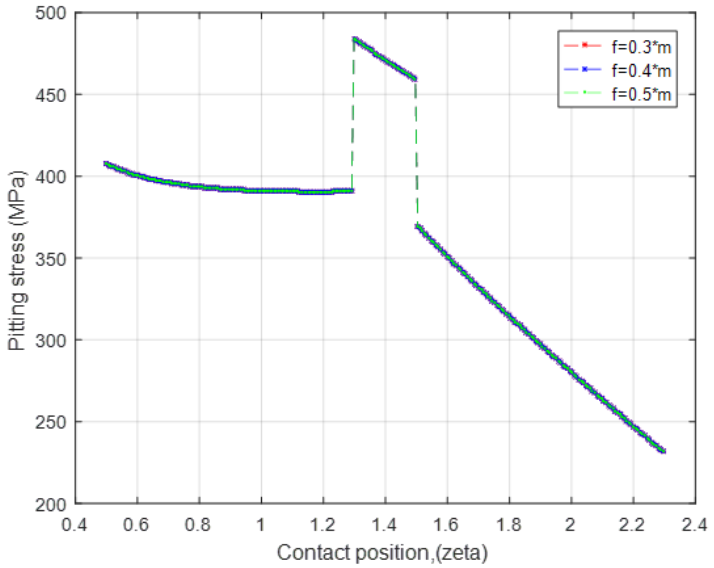

Fig. 9 Pitting stress along the pinion tooth

5.4. Case.3 Hertz's contact stress changes the pressure angles

The results showed that the stress distribution along the contact position was found at three different pressure angles. The distribution of pitting stress is slowly decreased at the base of gear tooth, the maximum pitting stress is occurred at the middle portion of the gear tooth, and the pitting stress is reduced at the tip of the gear tooth is shown in Figure 10. The gear failure occurs at the middle portion of the gear tooth because the maximum pitting stress appears in this position. If the pressure angle is increased, the maximum pitting stress along the pinion tooth is constant but maximum pitting stress position is increased. The gear failure occurs at an increase in the pressure angle.

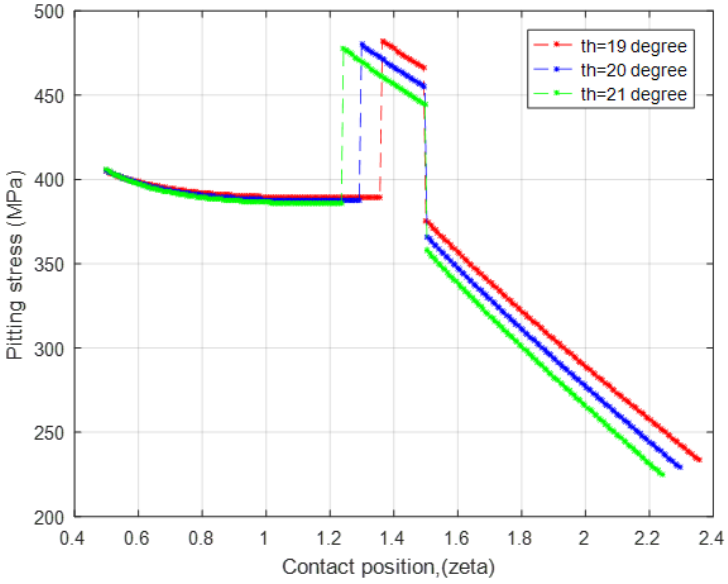

Fig.10 Pitting stress along the pinion tooth

6. AGMA Contact stress

Two fundamental stress equations are used in the AGMA methodology (i) Bending stress and (ii) Pitting resistance (contact stress). Pitting resistance can be calculated as follow:

$$\sigma_c = Z_E \sqrt{\frac{F_t.K_O.K_V.K_H.K_S.Z_R}{d_p.b.Z_I}} \tag{9}$$

Where, σ_c is the pitting resistance (contact stress) (MPa)

Z_E is the elastic coefficient ($\sqrt{MPa}$)

F_t is the transmitted tangential load (N)

K_O is the overload factor

K_V is dynamic factor

K_H is the load distribution factor

K_S is the size factor

Z_R is the surface condition factor for pitting resistance (Z_R =1)

d_p is the pitch circle diameter of pinion(mm)

b is the face width of the tooth(mm)

Z_I is the geometry factor for pitting resistance

$$Z_E = \left[\frac{1}{\pi\left(\frac{1-\upsilon_1^2}{E_1} + \frac{1-\upsilon_2^2}{E_2} \right)} \right]^{1/2} \tag{10}$$

6.1. Case 1 AGMA contact stress changes the modules

The results showed that the AGMA stress distribution along the contact position was found in three different modules. The distribution of AGMA contact stress is slowly increased at the base of the gear tooth, the maximum contact stress exists at the middle portion of the gear tooth, and the contact stress is reduced at the tip of the gear tooth is shown in Figure 11. The gear failure occurs at the middle portion of gear tooth because the maximum contact stress appears in this position. If the module increases, the contact stress along the pinion tooth is reduced. The failure of gear teeth can be reduced in the case of increased the module as it will adjust the hole of the gear and shaft diameter.

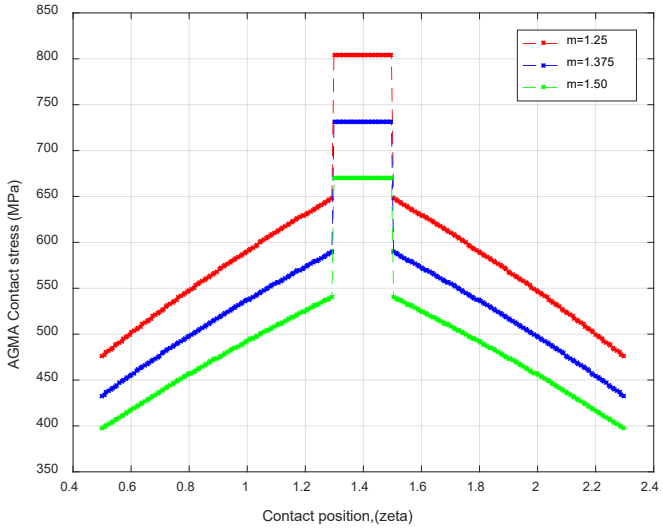

Fig.11 AGMA contact stress along the pinion tooth

6.2. Case 2 AGMA contact stress changes the addendum factor

The results showed that the AGMA contact stress distribution along the contact position was found in three different addendum factors. The distribution of contact stress is slowly increased at the base of the gear tooth, the maximum contact stress occurs at the middle portion of the gear tooth, and the AGMA contact stress reduces at the tip of the gear tooth is shown in Figure 12. The gear failure occurs at the middle portion of the gear tooth because the maximum pitting stress appears in this position. If the addendum factor increases, the maximum contact position can be reduced, although the AGMA contact stress along the pinion tooth is constant.

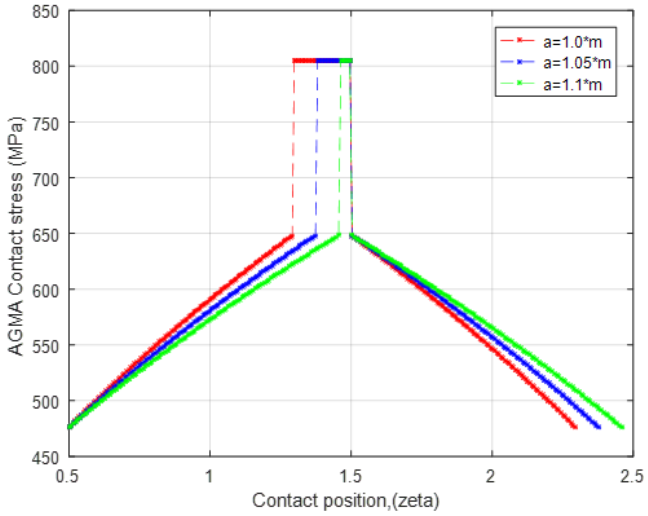

Fig.12 AGMA contact stress along the pinion tooth

6.3. Case 3 AGMA contact stress changes the fillet radius

The results showed that AGMA contact stress distribution along the contact position was found in three different fillet radii. The distribution of AGMA contact stress is slowly increased at the base of the gear tooth, the maximum contact stress occurs at the middle portion of the gear tooth, and the AGMA contact stress reduces at the tip of the gear tooth is shown in Figure 13. Although the fillet radius is increasing, the AGMA contact stress along the pinion tooth is constant.

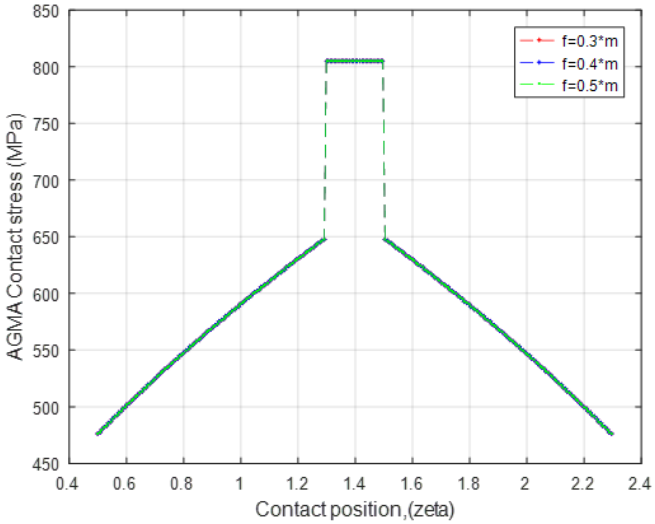

Fig.13 AGMA contact stress along the pinion tooth

6.4. Case 3 AGMA contact stress changes the pressure angles

The results showed that the AGMA contact stress distribution along the contact position was found in three different pressure angles. The distribution of AGMA contact stress is slowly increased at the base of the gear tooth, the maximum contact stress occurs at the middle portion of the gear tooth, and the AGMA contact stress is reduced at the tip of the gear tooth is shown in Figure 14. The gear failure occurs at the middle portion of the gear tooth because the maximum contact stress appears in this position. If the pressure angle is increased, the maximum contact stress along the pinion tooth is constant but the maximum pitting stress position is increased. The gear failure occurs when an increase in pressure angle.

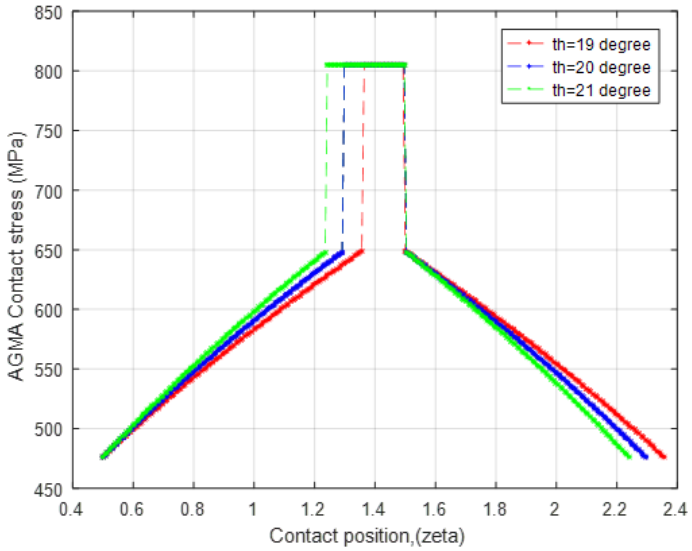

Fig.14 AGMA contact stress along the pinion tooth

7. Allowable contact stress

AGMA allowable stress number (strength) for contact stress for

$$S_c = (2.22H_B + 200)\,\text{MPa} = 890.42\,\text{MPa} \quad (11)$$

The results of Hertz contact stress, AGMA contact stress and allowable contact stress are expressed in Table.3.

Table.3. Contact stress for four different cases

Case	Name	Max: Hertz's contact stress (MPa)	Max: AGMA contact stress (MPa)	Max: Allowable contact stress (MPa)
1	Module(m=1.5)	410	670	890.42
2	Addendum factor(a=1.1*m)	480	800	890.42
3	Fillet radius(all)	480	800	890.42
4	Pressure angle (α= 19°)	480	800	890.42

Table 3. shows the maximum contact stress at the highest point of single tooth contact (HPST). The contact stress is minimum in the case of module is increased, It will be needed to adjusted the shaft diameter because it is increased the weight of gear. Although the maximum contact stress is the same, the failure position is reduced in the case of the addendum factor is increased. As the maximum contact stress is the same, the failure position is same in the case of the fillet radius is increased. The contact stress is not depended in the case of the fillet radius is increased. Although the maximum contact stress is the same, the failure position is reduced in the case of the addendum factor is decreased.

8. Conclusion

First, the accurate profile equation of an involute spur gear is established to formulate a new analytical model for the maximum load distribution and the pitting stress calculations based on the mechanics theory. Then, the maximum load distribution and the contact stress(pitting stress) of the new model in Case 1–4 with different normal modules ,addendum factor, fillet radius and normal pressure angles were calculated and compared to that of the Hertz's model by numerical calculation, and the AGMA model based on the gear strength. In addition, the error of the maximum contact stress between the new models of increase the addendum factor is the smallest. Although, the maximum contact stress is minimum in the case of increase the module but it will be needed to adjust the shaft diameter.

Reference

[1]. J.I.Pedrero,M.Pleguezuelos,M.Artes,J.A.Antona, Load distribution model along the line of contact for involute external gears, Mechanism and .Machine Theory 45(2010) 780-794.
[2]. M.B.Sanchez, M.Pleguezuelos, J.I.Pedrero, Enhanced model of load distribution along the line of contact for non-standard involute external gears, Meccanica 48(2011)527-537.
[3] Q.Wang,Y.Zhang,A model for analyzing stiffness and stress in a helical gear pair with tooth profile errors, J.Vib.Control(2015).
[4] G.B.Ingole, S.B.Wadkar, D.S.Watwisave, Analysis of stress relieving features of asymmetric spur gear, International Journal of Innovation in Engineering, Research and Technology [IJIERT] ICITDCEME'15 Conference Proceedings ISSN No - 2394-3696.
[5] https://adamant-precision.ch/blog/importance_of_contact_ratio.
[6] AGMA standard 2001-D04, American Manufactures Association Alexandria.VA.2004.
[7] Miryam B. Sánchez, Miguel Pleguezuelos, José I. Pedrero, Approximate equations for the meshing stiffness and the load sharing ratio of spur gears including hertzian effect, Mechanism and Machine Theory 109(2017) 231-249.